Infrastructure Management, Assessment and Rehabilitation

Infrastructure Management, Assessment and Rehabilitation

Edited by

Sherif Yehia, Mahmoud Reda Taha
and Akmal Abdelfatah

Cambridge Scholars Publishing

Infrastructure Management, Assessment and Rehabilitation

Edited by Sherif Yehia, Mahmoud Reda Taha and Akmal Abdelfatah

This book first published 2021

Cambridge Scholars Publishing

Lady Stephenson Library, Newcastle upon Tyne, NE6 2PA, UK

British Library Cataloguing in Publication Data
A catalogue record for this book is available from the British Library

ISBN (10): 1-5275-6947-0
ISBN (13): 978-1-5275-6947-8

TABLE OF CONTENTS

Part III: System Management and Sustainability

PREFACE

The International Conference on Infrastructure Management, Assessment and Rehabilitation Techniques is an international event that has taken place every two years for the last decade. The conference provides a forum for scientists and engineers engaged in research and development to convene and present their latest work on infrastructure resilience, management, assessment, and rehabilitation techniques. Following two successful conferences, ICIMART'14 (2014) and ICIMART'16 (2016), ICIMART'19 was held March 5–7, 2019 at the American University of Sharjah (AUS), Sharjah, the United Arab Emirates. The ICIMART'19 theme focused on infrastructure resilience, rehabilitation and management, and innovative testing and methods for civil infrastructure.

ICIMART'19 brought together engineers, scientists, contractors, producers, and government agencies working in infrastructure management, assessment, and rehabilitation techniques. The three-day event featured 50 presentations, with 80 participants from 14 countries. The conference included five keynote speakers presenting state-of-the-art research on nano-modified 3D-printed concrete and composites, assessment and prediction of the performance of bridge decks, computer vision-based civil infrastructure maintenance, progress in marine concrete structures, engineering and construction of the Louvre Abu Dhabi, and the use of conductive concrete for electromagnetic shielding of a critical infrastructure facility. The conference was sponsored by Parsons, fib, Society of Engineers in the United Arab Emirates and the AUS College of Engineering. The conference proceedings include 25 top-quality peer-reviewed research papers presented at ICIMART'19, and is divided into five sections covering infrastructure resilience, infrastructure materials and methods, system management and sustainability, infrastructure analysis and design, and non-destructive evaluation techniques. Research work provides insight to owners, engineers, and contractors on a decision support system, the state of condition assessment of structures in the Middle East, and methods to improve infrastructure resilience. ICIMART'19 papers cover new advances on the use of special types of concrete, specially configured steel fibers to enhance shear strength of concrete, strain-hardening cementitious composites, and the use of recycled aggregate to produce pavements and new masonry units. Of particular interest are research papers discussing 3D-printed concrete and its application in constructing a new office building in Dubai. Interesting research also discusses the use of the significance of dynamic loadings on the structural design of bridges, a novel method for the design of I-girder bridges, non-contact wave estimation for predicting pavement distress, automated detection of defects using air-coupled impact echo, and the use of large-amplitude mobile shakers for damage identification in bridges. ICIMART'19 papers also examine the potential for technological advances to open up new frontiers using advanced carbon fiber composites to strengthen bridge deck slabs and reinforced concrete beams with shear cracks. The editors are confident the ICIMART'19 proceedings will provide the reader with an in-depth introduction to the state-of-the-art global research and development that is currently underway on infrastructure management, assessment, and rehabilitation techniques, and the diligent, innovative research paving the way toward sustainable and resilient infrastructure.

The Editors
Mahmoud Reda Taha, University of New Mexico, USA
Akmal Abdelfatah, American University of Sharjah, UAE
Sherif Yehia, American University of Sharjah, UAE

PART I:

INFRASTRUCTURE RESILIENCE

FIRE RESISTANCE OF SELF-COMPACTING HIGH-PERFORMANCE CONCRETE PRODUCED WITH CELLULAR CONCRETE POWDER

MOHAMMED ABED

Department of Construction Materials and Technologies
Műegyetem rkp 3. Budapest, H-1111, Hungary
abed.mohammed@epito.bme.hu

RITA NEMES

Department of Construction Materials and Technologies
Műegyetem rkp 3. Budapest, H-1111, Hungary
nemes.rita@epito.bme.hu

Abstract

The present experimental study investigates the impact of incorporating recycled coarse aggregate (RCA) and waste cellular concrete powder (WCCP) on the residual mechanical properties of self-compacting high-performance concrete (SCHPC) after exposure to elevated temperatures. Nine mixtures of SCHPC were produced by replacing the cement mass with 15% WCCP and 30% WCCP, respectively. In addition, the coarse natural aggregate (NA) was replaced by up to 50% of RCA. The fire resistant properties of SCHPC were enhanced by replacing the amount of cement with up to 15% of WCCP at temperatures higher than 500 °C. However, using 25% or 50% of RCA in the cement enhanced the fire resistance of SCHPC because of the strong aggregate-mortar contact zone and the similarity of thermal expansion between the two. Sustainable products could be produced by incorporating waste materials into the production of concrete, thus reducing waste materials, emissions of CO2 and the energy required for processing.

Keywords: self-compacting high-performance concrete, recycled concrete aggregate, waste cellular concrete powder, fire resistance, residual mechanical properties

1. Introduction

The investigations of researchers into recycling demolition waste conclude that the substance can be used to replace coarse natural aggregate (NA), thus paving the way for its use in the present, by unlocking the reuse of construction and demolition (C&D) waste and promoting the use of coarse recycled concrete aggregate (RCA) in new and different concrete types. Various materials have become a necessity for a sustainable, green and innovative future. Investigations in late 2017 into hundreds of research papers about RCA concluded that the use of mineral admixtures could enhance the properties of recycled aggregate concrete (RAC) (Kisku et al., 2017). Recommendations were made to conduct additional research into the addition of unconventional waste materials as cement replacement materials (CRMs) in addition to considering the long-term behavior of RAC with respect to its mechanical and durability properties. Several waste materials that were used as CRMs have been investigated (Meyer, 2009). It was concluded that the use of RCA, with the addition of an appropriate percentage of industrial waste, could be highly beneficial.

The use of unprocessed waste powder materials, such as CRMs, could provide more sustainable products from the point of view not only of reducing waste materials but also of emissions of carbon dioxide and the energy needed for processing (Limbachiya et al., 2012; Abed and Nemes, 2017). However, it was felt that these waste materials might be found to have either a positive, or negative effect on the mechanical behaviour of concrete after laboratory exposure to elevated temperatures (Cree et al., 2013). The main objective of the present study is to investigate the effect of elevated temperatures on the residual compressive and flexural strengths of SCHPC when RCA is incorporated into cement as a partial replacement for NA and WCCP. The fire resistance of SCHPC produced by incorporating waste materials is limited in any discussions on the topic in academic literature. However, discussion of fire resistance defined as “the ability of components of the building to perform their intended load-bearing functions under fire exposure” is more frequent (Novak and Kohoutkova, 2018).

2. Materials

2.1 Cement and waste cellular concrete powder

The cement used to conduct the present study was a Portland cement (CEM I 42.5N) which conformed to MSZ EN 197-1:2000 standards. It was used because of its ability to eliminate the effects of mineral admixtures of manufactured cement for testing and to show the impact on the mixture when Waste Cellular Concrete Powder (WCCP) is used as a partial replacement for the cement. The waste material was collected from a factory in Ytong that cuts cellular concrete masonry for use in Hungary (Xella Magyarország Kft.).

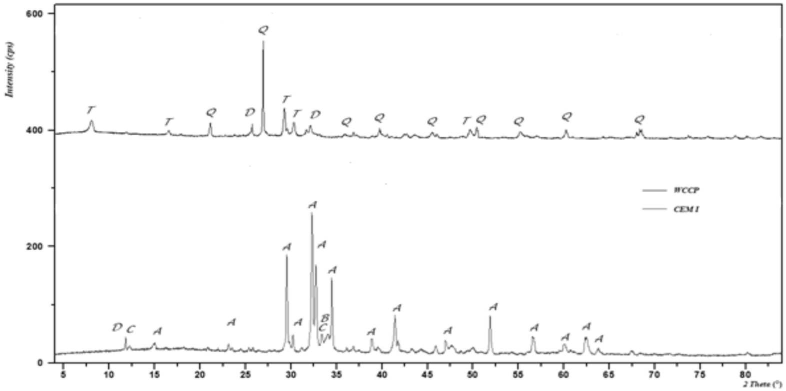

Fig. 1 X-ray Diffraction Profile for Cement and WCCP

The oxidizing composition was determined through the use of chemical analytical methods. The X-ray diffraction profiles for cement and WCCP are shown in **Fig. 1**. The data collected shows the chemical compositions and physical properties of the cement and waste powder materials (**Table 1)**. They were tested in accordance with MSZ EN 196-2:2013 and MSZ EN 525-12:2014 standards. **Fig. 2** shows the sieve curves for both cement and WCCP. The crystalline phases were identified as:

1. Cement (CEM I): Ca_3SiO_5 (C_3S, alite, hatrurite) as the main crystalline component; Ca_2SiO_4 (C_3S, belite, larnite) – its presence cannot be excluded; $CaSO_4.2H_2O$ (CSH_2, gypsum); $Ca_4Al_2Fe_2O_{10}$ (C_4AF, brownmillerite)
2. WCCP: alpha-SiO_2 (S, alpha-quartz) as the main crystalline component; $CaSO_4$ (CS, anhydrite) – hydrated mineral, called tobermorite. Note: 11A seems to explain several diffraction peaks.

Table 1 Chemical Composition and Physical Properties of Cement and WCCP

Measured property	*CEM I*	*WCCP*
Density (g/cm^3)	3.02	1.96
Specific surface area (cm^2/g)	3326	2513
Loss on ignition	3.0	9.25
SiO_2	19.33	54.28
CaO	63.43	22.81
MgO	1.45	1.15
Fe_2O_3	3.42	2.16
Al_2O_3	4.67	5.09
SO_3	2.6	4.90
Chloride content	0.04	0.02
Free CaO	0.71	–
Insoluble part in dilute hydrochloric acid and sodium carbonate	0.26	33.02

Fig. 2 illustrates the sieve curves for cement and WCCP. These indicate that WCCP has larger grain distributions than cement.

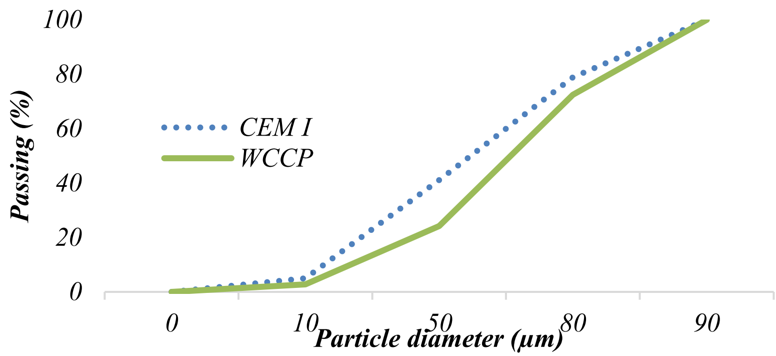

Fig. 2 Grading Curves of Cement and WCCP

2.2 Aggregates

Two types of aggregate were used in the present study:

1. Quartz sand and gravel (0/16 mm size), which were imported with two nominal grading fractions: sand (0/4 mm) and gravel (4/16 mm). The proportion of these was 45% and 55% respectively, in accordance with the optimal mix proposed by the authors.
2. Coarse recycled concrete aggregate (RCA), which was produced with the fraction of 4/16 mm. This was obtained by crushing concrete cubes with an average compressive strength between 28 and 33 MPa.

The RCA substitution rates of NA by mass were 0%, 25% and 50%, respectively. Both aggregates were tested to meet the requirements of BS EN 12620:2002+A1:2008. The grading curves of sand, NA and RCA are presented in **Fig. 3.** The water absorption capacity of RCA was 5.6%, due to the adhered mortar. It was used in air-dry situations. Extra water was added to compensate for the water absorption capacity.

3. Concrete mixtures

Nine SCHPC mixtures were produced through three series of tests. The main difference between the three was the substitution ratios of NA by RCA. In addition, in each series, the cement mass was partially replaced by WCCP mass. The amounts were 15% and 30%, respectively. **Table 2** shows the three mixtures produced in those series for this study.

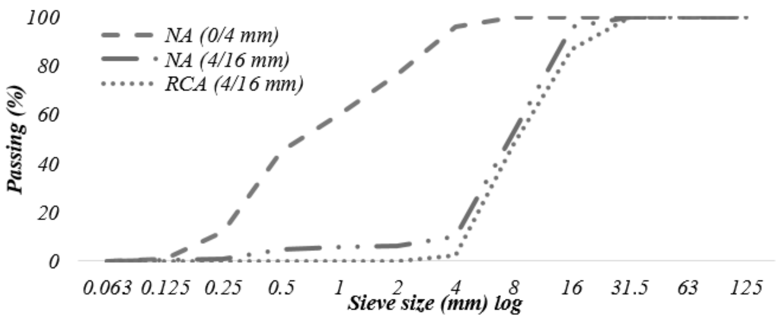

Fig. 3 Grading Curves of NA and RCA

Table 2 Mixing Series

Replacement of cement	Series I 0% replacement of coarse aggregate with RCA	Series II 25% replacement of coarse aggregate with RCA	Series III 50% replacement of coarse aggregate with RCA
0%	RA0	RA25	RA50
15% WCCP	C15RA0	C15RA25	C15RA50
30% WCCP	C30RA0	C30RA25	C30RA50

The water to binder ratio, was 0.35 for all mixtures, with a constant binder amount of 500 kg/m^3. This relatively low ratio content was selected due to the high performance results of the resulting concrete. At the same time, a considerable amount of the superplasticizer was used to achieve self-compacting. The water that was used in the mixture was tap water which complied with the requirements of BS EN 1008:2002. The proportions for all mixtures are shown in **Table 3**.

Table 3. Proportions in the Concrete Mix

Name of mixture	Proportions in kg/m^3						
	CEM I 42.5 N	WPP	Fine aggregate N. Sand 0/4	Coarse aggregate 4/16 NA	Coarse aggregate 4/16 RCA	superplasticizer	Water
	Series I: 0% RCA replacement						
RA0	500	0	783	939	0	1.5	175
C15RA0	425	75	766	919	0	1.7	175
C30RA0	350	150	750	899	0	3.25	175
	Series II: 25% RCA replacement						
RA25	500	0	783	704	230	1.5	175
C15RA25	425	75	766	690	225	1.7	175
C30RA25	350	150	750	674	220	3.25	175
	Series III: 50% RCA replacement						
RA50	500	0	783	470	460	1.5	175
C15RA50	425	75	766	459	451	1.7	175
C30RA50	350	150	750	451	442	3.25	175

4. Testing and heating procedure

The specimens were age-tested, under laboratory conditions at 95 ±5 days (three months), in accordance with RILEM recommendations. The specimens were heated to the maximum temperature for two hours, and then cooled down until the testing time, which was approximately 24 hours later.

The maximum temperatures were: 20 °C, 150 °C, 300 °C, 500 °C, 600 °C and 800 °C. A temperature range from 20 °C to 800 °C occurred for one hour – mirroring the temperature range which could occur in the case of a real fire (Hlavička, 2017). The heating curve was similar to the standard ISO 834 fire curve for buildings – that is up to 800 °C BS EN 1991-1-2:2002. Both compressive strength and 3-point flexural tests were carried out in order to determine the residual mechanical properties of the SCHPC specimens after they had been subjected to these elevated temperatures.

5. Results and discussion

5.1 Results at laboratory temperature

The consistency of the fresh SCHPC mixtures was tested by slump flow (slump diameter in cm) and V-Funnels (flow time in s). These were used to verify the achievement of the properties of the fresh mixture. All mixtures satisfied the European guideline for self-compacting concrete (EFNARC, 2005). The compression and flexural strengths were tested at ambient temperature at the aged rate of 90 days. In the case where RCA was incorporated, the strength-gaining rate was higher after 28 days (Rahal, 2007, Etxeberria et al., 2007, Kou and Poon, 2008). **Fig 4** shows the compressive and flexural strength results after a three-month period of aging for all nine of the SCHPC mixtures. All of the mixtures showed the same findings noted after the RCA dosage was increased to 50% of the compressive and flexural strengths. This is due to the good control of RCA grading as well as the high grade of the concrete (Kou and Poon, 2015, Abd Elhakam et al., 2012). Even when 15% of the cement was replaced by WCCP, the mix did not significantly change the mechanical properties of SCHPC. On the other hand, when up to 30% of the cement was replaced by WCCP, there was a significant deterioration in the mechanical properties of the SCHPC. All of the results were achieved at laboratory temperatures which have been published in other research papers by the authors of this paper (Abed & Nemes, 2017).

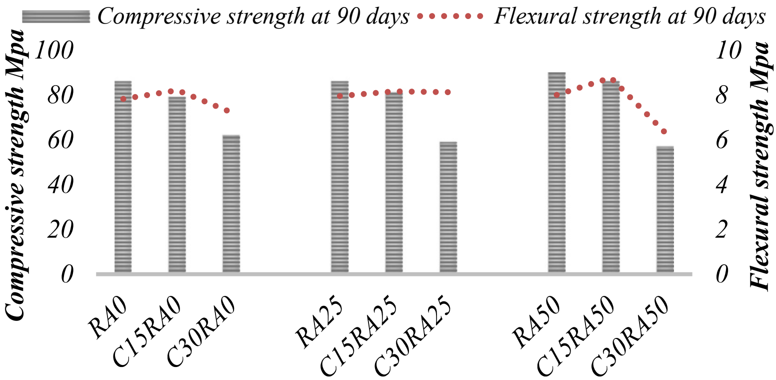

Fig. 4 Compressive and Flexural Strength at Laboratory Temperatures (90 days)

5.2 Results at elevated temperatures

The residual mechanical properties - the compressive and flexural strengths - which were taken after temperature elevations occurred are presented in this section. The properties were tested on day two of the 90-day study. Relative residual strength, as a function of temperature, is presented in this section. I^{st} is calculated by dividing the residual strength - which is taken after each degree rise in temperature - by the strength of the same mixture at ambient temperature. The relative residual strength is calculated separately for compressive and flexural strengths. These are called the relative residual compressive strength and the relative residual flexural strength.

Fig. 5 shows the development of the relative residual compressive and flexural strengths as a function of temperature. Three replacement amounts of NA by RCA are presented (RA0, RA25 and RA50). When RCA was used, SCHPC maintained higher residual strengths and behaved with the same tendency of reference as SCHPC. The same behavior has been observed for normal ordinary concrete (Schneider,1988). The positive effect of RCA is related to the strong ITZ bond between the adhered mortar of RCA and the new mortar, where two materials with the same composition (mortar to mortar) can give the same behavior at elevated temperatures. This similarity in behavior is attributed to the similar composition of both quartz aggregate and mortar: quartz aggregate has a higher facility to accommodate the differential at elevated temperatures (Zega and Di Maio, 2009).

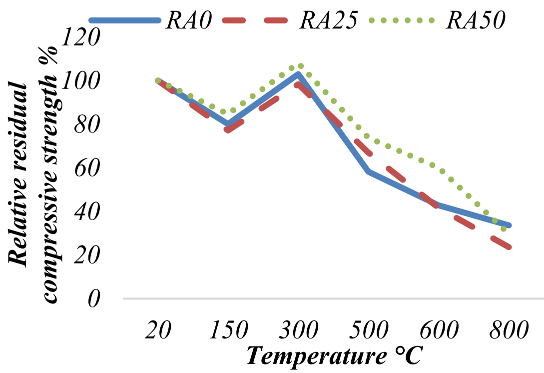

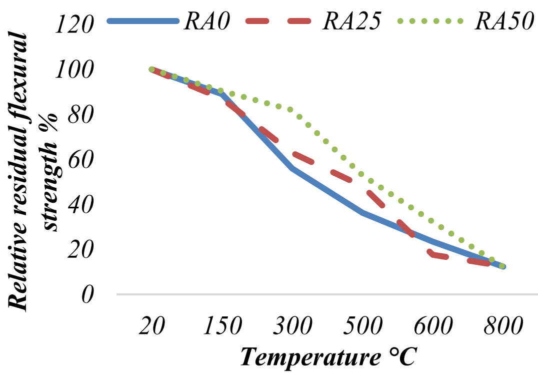

Fig. 5 Relative Residual Compressive and Flexural Strengths as a Function of SCHPC Temperatures (showing up to 50% RCA Replacement of NA)

As shown in **Fig. 6** and **Fig. 7**, the tendency of the relative residual compressive and flexural strengths of SCHPC as incorporated with WCCP was not specified and may vary from case to case. Findings in tests such as these indicate that the use of either RCA or NA is unfavorable. Furthermore, because WCCP has a high absorption capacity, higher temperatures are needed to eliminate it, along with relatively low amounts of CaO. Thus, WCCP enhances the fire resistance at high temperatures (higher than 400 °C).

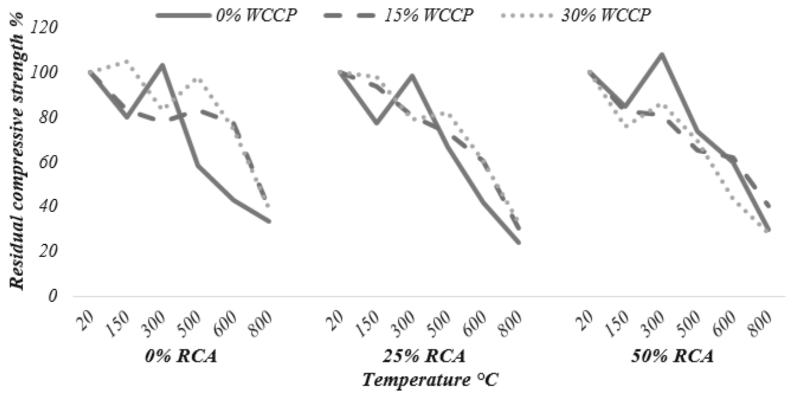

Fig. 6 Relative Residual Compressive Strengths as a Function of SCHPC Temperatures (showing up to 30% WCCP replacement of cement; up to 50% RCA replacement of NA)

This condition could be related to its composition. It contains a small amount of CaO, which enhances the fire resistance of concrete mixtures at high temperatures. It has been concluded that the low CaO/SiO_2 ratio of the binder means a higher relative residual compressive strength concrete after the thermal load of 800 °C (Lublóy et al., 2017). The ratios of the three main oxides of the cement and WCCP (SiO_2, CaO, Al_2O_3) are shown in **Table 4**. The results indicate that the CaO present in the WCCP is relatively low in comparison to the amount of SiO2. Thus, the positive effects of the RCA and the WCCP are more representative of the residual flexural strength versus the residual compressive strength, where the flexural strength has been enhanced by the incorporated RCA and/or WCCP at listed laboratory temperatures (shown in Figure 7).

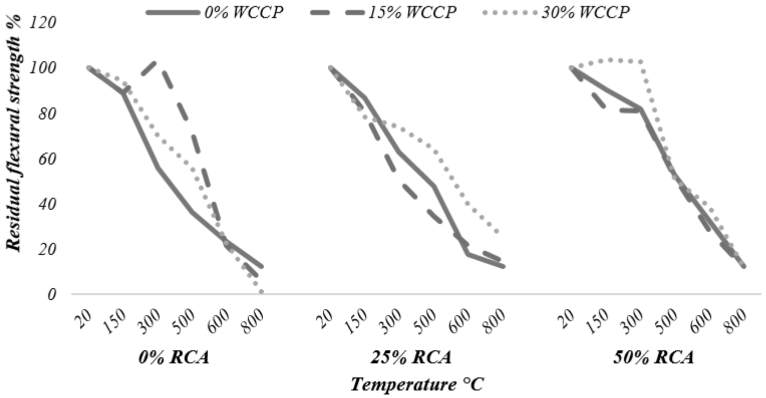

Fig. 7 Relative Residual Flexural Strengths as a Function of SCHPC Temperatures (showing up to 30% WCCP replacement of cement; up to 50% RCA replacement of NA)

Incorporating both RCA and WCCP into the SCHPC is an appropriate choice from the perspective of sustainability. In addition, a higher level of sustainable performance is indicated at elevated temperatures, with regard to the number of cracks and the amount of spalling.

Table 4: Ratios of 3 Main Oxides in Cement Composition

Powder material	***SiO_2***	***CaO***	***CaO/SiO_2***
CEM I	*20.21*	*66.31*	*328.14*
WCCP	*54.28*	*22.81*	*42.02*

6. Conclusion

The incorporation of waste and recycled materials in SCHPC offers not only sustainability but also an increased resistance for concrete structures under particular circumstances. The following conclusions can be drawn:

1. Increased RCA replacement positively affects the residual compressive and flexural strengths after temperature elevation. The replacement of NA by up to 50% RCA enhances the residual mechanical properties desired for a strong mortar-to-mortar bond.
2. The optimal replacement amount of cement by the WCCP as a function of the elevated temperature was 15%. The effectiveness of

the WCCP decreased in the case of the RAC, where the mortar-to-mortar bond was weakened due to large differences.

3. The WCCP positively affects fire resistance in temperatures that exceed 500 °C due to its superior ability to absorb water and its low CaO content. However, using a high proportion of WCCP is not recommended because it has been shown that mechanical properties deteriorate at laboratory temperatures and after raising the temperature in a degree-by-degree process.

Acknowledgement

The research reported in this paper was supported by the Higher Education Excellence Program of EMMI in the frame of the Water Sciences & Disaster Prevention Research area of BME (BME FIKP-VÍZ).

References

[1] ABD ELHAKAM, A., MOHAMED, A. E. & AWAD, E. (2012) Influence of self-healing, mixing method and adding silica fume on mechanical properties of recycled aggregates concrete. Construction and Building Materials, 35**,** 421-427.

[2] ABED, M. & NEMES, R. (2017) Possibility of Producing Green, Self-Compactin, High Performance Concrete (GSCHPC) – Review. Concrete Structures,, 18**,** 21-29.

[3] BS EN 12620:2002+A1 (2008) Aggregates for concrete.

[4] BS EN 1991-1-2 (2002) Eurocode 1: Actions on structures – Part 1–2: General actions – Actions on structures exposed to fire.

[5] BS EN 1008 (2002) Mixing water for concrete-Specification for sampling, testing and assessing the suitability of water, including water recovered from processes in the concrete industry, as mixing water for concrete.

[6] CREE, D., GREEN, M. & NOUMOWÉ, A. (2013) Residual strength of concrete containing recycled materials after exposure to fire: A review. Construction and Building Materials, 45**,** 208-223.

[7] EFNARC (2005) Specifications and guidlines for self-compacting concrete, English ed. European federation for specialist cinstruction chemicals &concrete systems.

[8] ETXEBERRIA, M., VÁZQUEZ, E., MARÍ, A. & BARRA, M. (2007) Influence of amount of recycled coarse aggregates and production process on properties of recycled aggregate concrete. Cement and Concrete Research, 37**,** 735-742.

[9] HLAVIČKA, É. L.-V. (2017) Bond after fire. Construction and Building Materials, 132, 210-218.
[10] KISKU, N., JOSHI, H., ANSARI, M., PANDA, S. K., NAYAK, S. & DUTTA, S. C. (2017) A critical review and assessment for usage of recycled aggregate as sustainable construction material. Construction and Building Materials, 131, 721-740.
[11] KOU, S. C. & POON, C. S. (2008) Mechanical properties of 5-year-old concrete prepared with recycled aggregates obtained from three different sources. Magazine of Concrete Research, 60, 57-64.
[12] KOU, S.-C. & POON, C.-S. (2015) Effect of the quality of parent concrete on the properties of high performance recycled aggregate concrete. Construction and Building Materials, 77, 501-508.
[13] LIMBACHIYA, M., MEDDAH, M. S. & OUCHAGOUR, Y. (2012) Use of recycled concrete aggregate in fly-ash concrete. Construction and Building Materials, 27, 439-449.
[14] LUBLÓY, É., KOPECSKÓ, K., BALÁZS, G. L., RESTÁS, Á. & SZILÁGYI, I. M. (2017) Improved fire resistance by using Portand-puzzolana of Portand fly ash cements. J. Therm. Anal. Calorim., 1, 1-12.
[15] MEYER, C. (2009) The greening of the concrete industry. Cement and Concrete Composites, 31, 601-605.
[16] MSZ EN 196-2 (2013) Cement testing methods. Part 2: Chemical analysis of cement.
[17] MSZ EN 197-1 (2000) Cement - Part 1: Composition, specifications and conformity criteria for common cements.
[18] MSZ EN 525-12 (2014) Chemical analysis of cement. Part 12: Determination of free lime content.
[19] NOVAK, J., & KOHOUTKOVA, A. (2018) Mechanical properties of concrete composites subject to elevated temperature. Fire Safety Journal 95 (Jan): 66– 76.
[20] RAHAL, K. (2007) Mechanical properties of concrete with recycled coarse aggregate. Building and Environment, 42, 407-415.
[21] SCHNEIDER, U. (1988) Concrete at high temperatures — A general review. Fire Safety Journal, 13, 55-68.
[22] ZEGA, C. J. & DI MAIO, A. A. (2009) Recycled concrete made with different natural coarse aggregates exposed to high temperature. Construction and Building Materials, 23, 2047-2052.

UNDERSTANDING DYNAMIC LOADING AS USED IN VIADUCT ELEVATED RAILWAYS FOR SUSTAINABLE DESIGN

MOHAMED WEHBI

National Design Team, Network Rail
Birmingham, United Kingdom
mohamed.wehbi@networkrail.co.uk

GHASSAN ABU-LEBDAH

Department of Civil Engineering, AUS
Sharjah, United Arab Emirates
gabulebdeh@aus.edu

Abstract

The use of viaduct-elevated railway systems has become more common in recent years. However, designers are faced with the unique challenge of how to account for the dynamic effects of moving trains in the design of viaduct railway structures. To overcome this challenge, designers resort to relationships shown to be available in the literature. These are listed as ballasted tracks, to estimate the dynamic loading. This approach can lead to over-design which may result in a high construction cost. This is because these relationships tend to recommend high degrees of dynamic loading due to the constructed nature of ballasted tracks. The aim of this paper is to investigate the effect of dynamic loading when moving trains are on viaduct railway structures by using numerical modelling. The study concluded that the dynamic behaviour of such structures is unique and if it is well understood it can lead to more sustainable designs.

Keywords: elevated railways, modelling, train-track interaction, dynamics, sustainability.

1. Introduction

The increased demand on transportation systems in over-populated cities, with restricted space, has pushed engineers to develop innovative solutions to enable the adaptation of conventional transportation systems to those cities. A great example of such an adaptation is the London Underground Rapid Railway System - the London Underground and Metropolitan Line, built in the late 18th century. When the Victorians invented the railway system, it was designed to transport goods and passengers between different cities. However, to be able to use the railways in the City of London, where the ability to build railway tracks was limited, engineers had to design a network of underground tunnels to allow tracks to be constructed underground (see Figure 1). Many cities in Europe use a similar approach. However, this approach proved to be extremely difficult and costly due to the unforeseen soil conditions encountered during excavation work. As a result, engineers started to adopt the concept of an elevated viaduct railway system, which uses a series of viaduct bridges to elevate the railway tracks above the surface of the ground (see Figure 2). Such systems operate in Kuala Lumpur and Dubai. However, a viaduct railway system has a major disadvantage associated with it in the understanding of full loading conditions; more specifically to train dynamic loading. To overcome this disadvantage, engineers resort to high factors of safety to compensate for any unknowns related to the dynamic effect of the train. However, this approach may lead to over-design and, consequently, considerable construction costs. Therefore, the aim of this paper is to investigate the effect of dynamic loading generated by moving trains on elevated viaduct railway systems. This will allow a better understanding of what factors of safety should be employed to take advantage of more sustainable designs and permit engineers to comprehend how to compare it to other industry practices. This is achieved with the aid of a 3D numerical model to simulate the stress and deformation generated due to train loading at static and dynamic (at various travel speeds) conditions.

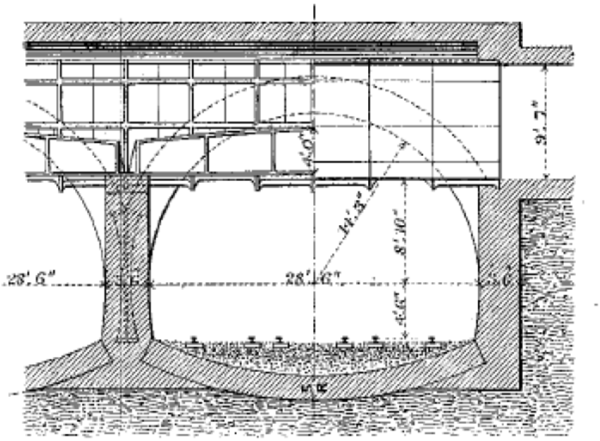

Figure 1: London Tube System (Jones, 2014)

Figure 2: Dubai Metro Viaduct System

2. Train dynamic loading

The structure of a railway track is designed to maintain a predetermined cumulative traffic load, i.e., design life with minimum maintenance. The cumulative traffic load is made up of repetitions of train induced load pulses or dynamic train loads. Dynamic train loads have been found to be a function of the condition and quality of the track, differential support (differential track stiffness), and train speed (Bezgin, 2017). If the surface of the rail is perfectly smooth, then the speed of the train will have little, or no effect on the total load applied. In reality, however, the surface is never smooth and surface irregularities can cause the wheels of the train to bounce vertically (see Figure 3). This is due to the inertial effect of the body of the train, which can significantly amplify the static load (Burrow et al, 2017).

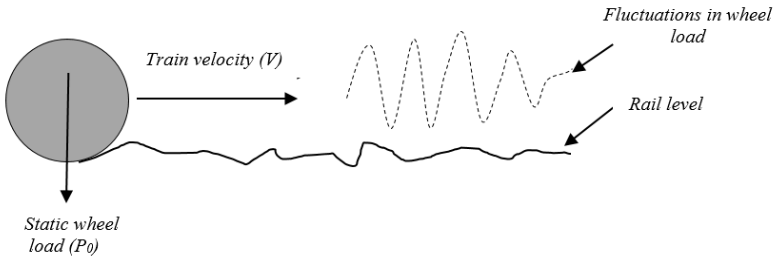

Figure 3: Effect of Track Irregularities on Wheel Load

Conventionally, and for design purposes, dynamic loads are related to static loads by a Dynamic Amplification Factor (DAF), in the form of Equation 1 (Stewart and O'Rourke, 1988).

$$P_d = DAF \times P_0 \qquad (1)$$

Where:

P_d: dynamic wheel load
DAF: Dynamic Amplification Factor
P_0: static wheel load

In an empirical study on ballasted railways carried out by Eisenman (1992), he found that for speeds up to 60Km/r the DAF followed a Gaussian distribution, which depended primarily on the geometry of the track, as shown in Equation 2. On the other hand, when the speed of the train exceeded 60Km/h the DAF was found to be dependent on both the train speed and the track geometry, as shown in Equations 2, 3 and Figure 4. It should be noted that it is common practice among designers to use a DAF value of 1.5 to develop track designs.

$$DAF = 1 + \varphi t \qquad \text{For V<60Km/h} \qquad (2)$$

$$DAF = 1 + \varphi t\left(1 + \frac{V-60}{140}\right) \qquad \text{For } 60 \leq V \leq 200\text{Km/h} \qquad (3)$$

Where:

φ: track geometry coefficient
- for very good track geometry $\varphi = 0.1$
- for good track geometry $\varphi = 0.2$
- for poor track geometry $\varphi = 0.3$

t: risk factor, varying from 1 to 3 depending on the design risk

V: train speed in km/h

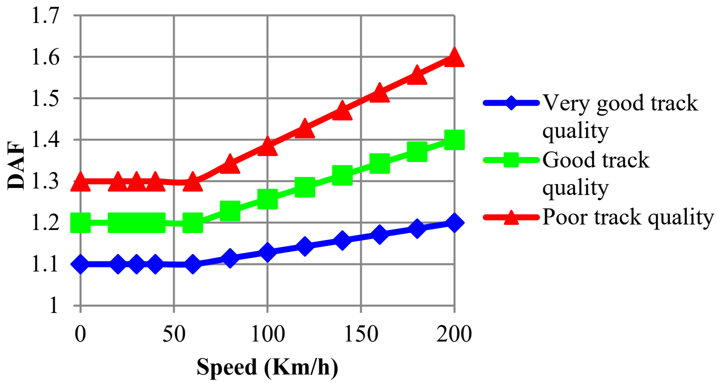

Figure 4: Effect of Track Geometry on DAF (based on Eisenman's (1977) model)

As for railway tracks specifically built on bridges and viaducts, several railway standards suggest different empirical relationships are used in estimating the dynamic effect on train loading as a function of bridge spans. This, of course, does not take into account the speed at which the train is traveling. For example, the AREMA (American Railway Engineering & Maintenance of Ways Association) manual suggests that the dynamic wheel force of the train can be estimated using only a bridge span as the input parameter, via Equations 4 and 5 (Rakoczy and Nowak, 2018). The lack of consideration of travel speed in these empirical relationships can sometimes lead to less sustainable bridge designs – due to over-estimation, or under-estimation.

$$DAF = 1 + \frac{(40 - \frac{3L^2}{1600})}{100} \qquad \textit{for } L<100ft \qquad (4)$$

$$DAF = 1 + \frac{(40 - \frac{3L^2}{1600})}{100} \qquad \textit{for } L\geq 100ft \qquad (5)$$

Where:

L is the effect span length in feet

3. Study frame of work

To investigate the effects of train dynamic loading on elevated railway viaduct structures, a 3D numerical dynamic model was developed to simulate the behaviour of the track system on viaducts under two different loading conditions: 1) static train loads 2) dynamic moving train loads (at different speeds: 40km/h; 80km/h; 120km/h;160km/h). In the dynamic loading condition, the train inertial forces as well as stress wave propagation are accounted for. On the other hand, the static load condition ignores these two parameters and assumes that equilibrium is achieved at each loading position on the track. This approach allows comparison between the dynamic and static responses to better inform designers on the appropriate value of DAF that should be used in the design of such structures at various train speeds. From the static and dynamic simulations, a number of performance indicators are assessed and compared, as seen with the following:

1. *Wheel dynamic load*: As discussed in the previous section, rail irregularities, differential track supports and train speeds can cause the wheel to bounce leading to fluctuations in the wheel-rail dynamic force. High dynamic forces can also lead to contact fatigue in the rail surface, which leads to cracks caused by Rolling Contact Fatigue (RCF). This can bring about rail breakage, resulting in high to high stresses along the concrete structures of the viaduct (Wehbi & Musgrave, 2017). On the other hand, low dynamic forces can impose serious safety considerations by increasing the risk of train derailment. The wheel dynamic load can be modelled using Hertzian contact theory, as shown in Equation 6 (Zhai et al., 2004; Sichani, 2013).

$$P_d(t) = \left[\frac{1}{G} \quad \Delta Z(t)\right]^{3/2} \qquad (6)$$